Measurements and predictive models of high-pressure H2 solubility in brine (H2O+NaCl) for Underground Hydrogen Storage application

Salaheddine Chabab, Pascal Theveneau, Pascal Théveneau, Christophe Coquelet, Jérôme Corvisier, Patrice Paricaud

Measurements and predictive models of high-pressure H_2 solubility in brine (H_2O+NaCl) for Underground Hydrogen Storage application

Salaheddine Chabab[a], Pascal Theveneau[a], Christophe Coquelet[a,]*, Jérôme Corvisier[b] and Patrice Paricaud[c,a]

[a]*Mines ParisTech, PSL University, Centre of Thermodynamics of Processes, 35 rue Saint Honoré, 77305 Fontainebleau Cedex, France*

[b]*Mines ParisTech, PSL University, Centre de Géosciences, 35 rue Saint Honoré, 77305 Fontainebleau Cedex, France*

[c]*Unité Chimie & Procédés (UCP), ENSTA Paris, 828 Boulevard des Maréchaux, 91762 Palaiseau cedex, France*

*Corresponding author. Tel: +33164694962, E-mail address: christophe.coquelet@mines-paristech.fr (C. Coquelet)

Journal:

International Journal of Hydrogen Energy

Abstract

In the context of Underground Hydrogen Storage (UHS), the stored gas is in direct contact with brine (residual brine from the cavern or formation water of deep aquifers). Therefore, knowledge of the phase equilibria (solubility of hydrogen in brine and water content in the hydrogen-rich phase) in the geological reservoir is necessary for the study of hydrogen mobility and reactivity, as well as the control, monitoring and optimization of the storage. The absence of measured data of high-pressure H_2 solubility in brine has recently led scientists to develop predictive models or to generate pseudo-data using molecular simulation. However, experimental measurements are needed for model evaluation and validation. In this work, an experimental apparatus based on the "static-analytic" method developed and used in our previous work for the measurement of gas solubility in brine was used. New solubility data of H_2 in H_2O+NaCl were measured more or less under the geological conditions of the storage, at temperatures between 323 and 373 K, NaCl molalities between 0 and 5m, and pressures up to 230 bar. These data were used to parameterize and evaluate three models (Geochemical, SW, and e-PR-CPA models) tested in this work. Solubility and water content tables were generated by the e-PR-CPA model, as well as a simple formulation (Setschenow-type relationship) for quick and accurate calculations (in the fitting range) of H_2 solubility in water and brine was proposed. Finally, the developed models estimate very well the water content in hydrogen-rich phase and capture and calculate precisely the salting-out effect on H_2 solubility.

Keywords: H_2 solubility, water, brine, Underground Hydrogen Storage, Electrolyte CPA EoS, Measurement, Modeling

1. Introduction

Hydrogen (H_2) is considered to be a renewable energy carrier with promising prospects for energy transition. It can be used directly in fuel cells for transport and mobility applications, or as a complement to existing energy resources such as the production of synthetic methane by combining it with CO_2 through methanation, and the injection into existing Natural Gas (NG) networks with the aim of reducing consumption (in the short term) and stopping the use (in the long term) of fossil fuels. To manage the intermittent nature of renewable energy sources such as wind and solar power, surplus electricity can be stored in chemical form by producing H_2 through water electrolysis (power-to-gas concept). In order to balance the temporal differences between production and demand, storage of pure or blended (e.g. with NG [1, 2]) hydrogen is necessary.

Hydrogen can be stored in gaseous form in gas cylinders, in liquid form in cryogenic tanks, or in solid form by adsorption, absorption or by reacting with some chemical compounds [3]. However, the most studied and used technology for hydrogen large-scale storage is underground storage in geological formations such as salt caverns, deep aquifers, and depleted gas fields. In addition to their huge storage capacity (in terms of volume and pressure), underground hydrogen storage remains more cost-effective and safer than other storage techniques [4, 5].

Hydrogen storage in salt caverns has been done successfully for decades. However, none of this storage has been done for energetic purposes, since the stored hydrogen was mainly dedicated to the chemical and petrochemical industry. Large quantities of hydrogen are used [6] in refineries (50%) to remove/recover sulfur from fuels using hydrotreating (hydrogenation process), and in the Haber process (32%) for ammonia (NH3) synthesis by combining nitrogen (N2) and hydrogen (H2). Currently, four sites for hydrogen storage in salt caverns are operational worldwide: three in the USA (Clemens Dome, Moss Bluff, Spindletop) and one in the UK (Teesside). Several projects are in progress or have just been completed studying for energy purposes the storage of pure hydrogen in salt caverns (H2STORE, HyUnder, HyStock, Rostock H, STOPIL H2, etc.) and in gas fields (SunStorage and HyChico projects) or possibly mixed with CO_2 in deep saline aquifers (Underground bio-methanation concept [7]) or with CH_4 (SunStorage and HyChico projects). A benchmarking study of the different options for high-pressure hydrogen storage was carried out as part of the European project HyUnder [8]. This comparative study concluded that, according to the different techno-economic and safety

factors, storage in salt caverns is first in the ranking, followed by storage in depleted gas fields and storage in deep saline aquifers. Finally, hydrogen (especially pure) storage in salt caverns is preferred for several reasons [9]: the least expensive of all forms of storage, less cushion gas than storage in porous media, the possibility of several injection/withdrawal cycles, and a positive experience feedback.

Underground Hydrogen Storage (UHS) is much less studied than the underground natural gas storage, therefore in most existing hydrogen storage sites, the pressure does not exceed more or less than 150 bar. This is explained by its high mobility due to its small size [10], as well as its high reactivity (redox reactions) by possibly participating in certain microbial processes: sulfate-reduction, methanogenesis, acetogenesis, and iron-reduction [11, 12]. Most of these types of reactions can take place in the aqueous medium, i.e. in the residual brine after the solution mining of salt caverns or in the formation water of deep aquifers. The study of the mobility and reactivity of hydrogen is therefore necessary for the total control of the storage of this molecule, as well as for the reduction of the safety factors used (just by feedback), and consequently a more efficient and economical storage. In order to be able to perform chemical speciation calculations and study its mobility, it is therefore necessary to determine precisely the solubility of hydrogen in the aqueous phase under the thermodynamic storage conditions (temperature, pressure and salinity). Finally, the simulation and control of storage facilities, as well as the monitoring of hydrogen (temperature, pressure and quantity) in the reservoir (salt cavern or aquifer), requires knowledge of phase diagrams (solubility and water content of hydrogen) [13].

The solubility of hydrogen in water has been extensively studied at different pressures (P) and temperatures (T) in the past, as well as in saline water only under atmospheric P−T conditions. However, there are no high-pressure data of hydrogen solubility in saline water [14]. This can be justified by the complexity and dangerousness of this type of measurements, which are characterized by high pressure, high flammability of H_2, and presence of salt (risk of corrosion and leakage). To overcome this lack of data, recently “predictive” models adjusted on a limited number of data (available experimental data and/or molecular simulation data) have been proposed. Li et al. [15] proposed a model to predict the solubility of hydrogen in brine under geological storage conditions. The parameters of their model were adjusted on H_2 solubility data in brine at atmospheric pressure and high-pressure H_2 solubility data in pure water. Lopez-Lazaro et al. [13] performed Monte Carlo simulations to generate pseudo-experimental data, which were then correlated using an equation of state (Soreide and Whitson model [16]). An

inconsistency between the two studies was identified, which was totally expected, given the different approaches used and the lack of experimental data. However, further experimental measurements are needed to evaluate these predictions and refine existing models by including "real" high-pressure solubility data.

In this work, the solubility of hydrogen in brine (H_2O+NaCl) was measured analytically with the apparatus used in our previous work on the carbon dioxide and oxygen solubility in brine [17, 18]. The measurements were carried out more or less under the geological storage conditions (temperature $323 \leq T\,(K) \leq 373$, pressure up to 200 bar and NaCl molality $0 \leq m_{NaCl}$ (mol/kgw) ≤ 5). These new data, as well as existing literature data, were used to parameterize the models developed and presented in our previous work [17, 18] using different thermodynamic approaches (gamma-phi and phi-phi).

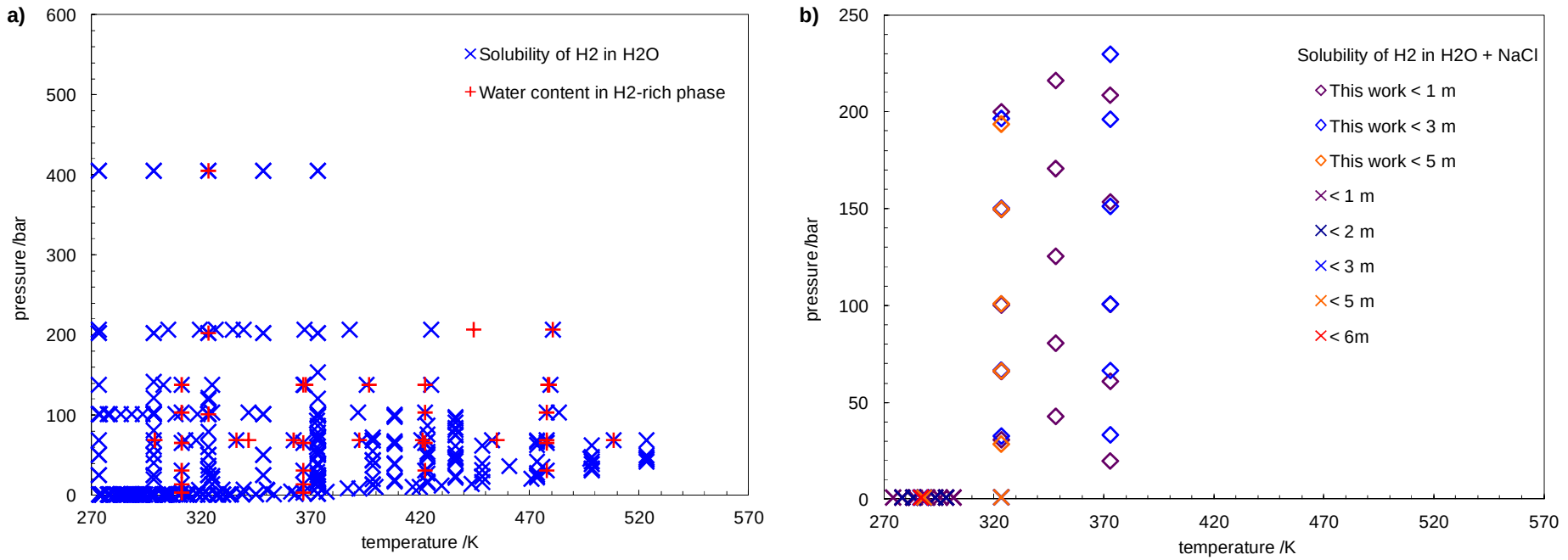

Figure 1 : Distribution of literature solubility data (×) and this work (◊). (a): H_2-H_2O system (solubility and water content); (b): H_2 solubility in NaCl brine.

2. Experimental

2.1. Literature and measured (this work) solubility data of H_2 in water and brine

In the literature, there are numerous data on the solubility of hydrogen in pure water, the majority of which come from very old studies. These data were collected, listed in Table 1, and presented in Figure 1.a as function of temperature and pressure. The Wiebe and Gaddy [19] data are the most reliable according to IUPAC's [20] evaluation of experimental data, and largely cover the pressure and temperature range of geological storage conditions.

The solubility of hydrogen in brine is less studied than in pure water. In Table 2, hydrogen solubility data in water + salt (NaCl, KCl, $CaCl_2$, Na_2SO_4 and $MgSO_4$) are listed. All these data found are old and limited to low temperature and atmospheric pressure. It is therefore necessary to overcome this lack of data especially for the H_2+H_2O+NaCl system which is the most important since Na^+ and Cl^- are the predominant species present in natural saline water. The measurements carried out in this work for the H_2+H_2O+NaCl system as well as data from the literature are presented in Figure 1.b as function of temperature, pressure and NaCl molality.

Table 1 : Literature experimental data for H_2 solubility in pure water

Reference	Year	Tmin/K	Tmax/K	Pmin/bar	Pmax/bar
Bunsen [21]	1855	277.15	296.75	1.021	1.042
Timofejew [22]	1890	274.55	298.85	1.020	1.046
Bohr and Bock [23]	1891	273.20	373.15	1.019	2.030
Winkler [24]	1891	273.65	323.25	1.020	1.138
Steiner [25]	1894	288.20	288.20	1.030	1.030
Braun [26]	1900	278.15	298.15	1.022	1.045
Geffcken [27]	1904	288.15	298.15	1.030	1.045
Knopp [28]	1904	293.15	293.15	1.037	1.037
Hufner [29]	1907	293.15	293.34	1.037	1.037
Findlay and Shen [30]	1912	298.15	298.15	1.009	1.840
Muller [31]	1913	289.35	290.35	1.032	1.033
Ipatiew et al. [32]	1932	273.65	318.15	20.265	141.855
Wiebe and Gaddy [19]	1934	273.15	373.15	25.331	1013.250
Morrison and Billett [33]	1952	285.65	345.65	1.028	1.350
Pray et al. [34]	1952	324.82	588.71	6.900	24.150
Zoss [35]	1952	273.15	606.48	34.500	207.000
Pray and Stephan [36]	1953	373.15	435.93	14.133	100.308
Wet [37]	1964	291.65	304.55	1.035	1.059
Ruetschi and Amlie [38]	1966	303.15	303.15	1.056	1.056
Shoor et al. [39]	1969	298.15	333.15	1.045	1.213
Longo et al. [40]	1970	310.15	310.15	1.076	1.076

Power and Stegall [41]	1970	310.15	310.15	1.076	1.076
Gerecke and Bittrich [42]	1971	298.15	298.15	1.045	1.045
Jung et al. [43]	1971	373.15	423.15	9.962	85.844
Schroder [44]	1973	298.15	373.15	101.300	101.300
Crozier and Yamamoto [45]	1974	274.60	302.47	1.013	1.013
Gordon et al. [46]	1977	273.29	302.40	1.013	1.013
Cargill [47]	1978	277.70	344.83	1.022	1.350
Gillespie and Wilson [48]	1980	310.93	588.71	3.450	138.000
Choudhary et al. [49]	1982	323.15	373.15	25.331	101.325
Dohrn and Brunner [50]	1986	473.15	623.15	100.000	300.000
Alvarez et al. [51]	1988	318.90	497.50	4.360	45.940
Kling and Maurer [52]	1991	323.15	423.15	31.800	153.700
Jauregui-Haza et al. [53]	2004	353.00	373.00	1.486	2.025

Table 2 : Literature experimental data for H_2 solubility in saline water

Reference	Year	Max Molality	Tmin/K	Tmax/K	Pmin/bar	Pmax/bar
Steiner [25]	1894	5.3 m NaCl	286.32	286.95	1.028	1.029
Braun [26]	1900	1.1 m NaCl	278.15	298.15	1.022	1.045
Gerecke & Bittrich [42]	1971	4.3 m NaCl	288.15	298.15	1.030	1.045
Crozier & Yamamoto [45]	1974	0.5 m NaCl	274.03	301.51	1.013	1.013
Steiner [25]	1894	4.0 m KCl	291.77	292.38	1.035	1.036
Knopp [28]	1904	2.1 m KCl	293.15	293.15	1.037	1.037
Gerecke et Bittrich [42]	1971	1.0 m KCl	288.15	288.15	1.030	1.030
Steiner [25]	1894	3.2 m $CaCl_2$	290.83	291.67	1.034	1.035
Steiner [25]	1894	1.4 m Na_2SO_4	291.56	291.72	1.035	1.035
Steiner [25]	1894	2.6 m $MgSO_4$	290.25	291.41	1.033	1.034

2.2. Materials

In Table 3, the suppliers of Hydrogen (H_2, CAS Number: 1333-74-0) and Sodium Chloride (NaCl, CAS Number: 7647-14-5) and the given purities are listed. Water was deionized and degassed before the preparation of the brine (water + NaCl).

Table 3 : Chemicals used in this work: purities and suppliers

Chemicals	Purity	Analytical Method	Supplier
H_2 (Hydrogen 5.0)	99.999 vol%	GC: Gas Chromatography	Messer
NaCl	99.6%	None	Fisher Chemical

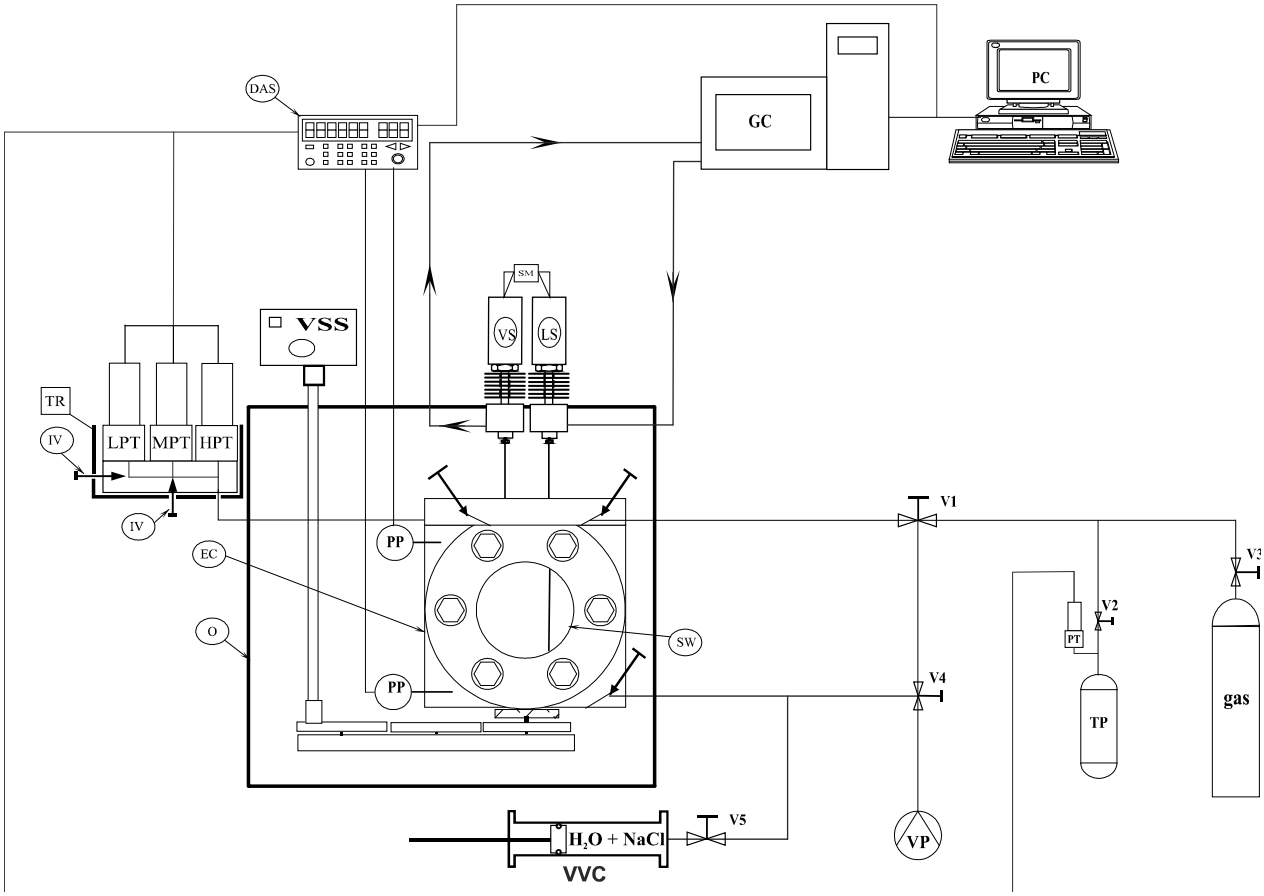

Figure 2 : Schematic representation of the static-analytic apparatus [17] used to measure the solubility of gas (H_2) in NaCl brine. DAS: data acquisition system, EC: equilibrium cell, GC: gas chromatography, HPT: high pressure transducer, LPT: low pressure transducer, LS: liquid ROLSI® capillary Sampler-Injector, MPT: medium pressure transducer, O: oven, PP: platinum resistance thermometer probe, PT: pressure transducer, IV: homemade shut off valve, SM: samplers monitoring, SW: sapphire window, TP: thermal press, TR: temperature regulator, Vi: valve i, VP: vacuum pump, VS: vapor ROLSI® capillary Sampler-Injector, VSS: variable speed stirrer and VVC: Variable Volume Cell.

2.3. Apparatus and method

The experimental method used for this work has already been employed to measure the solubility of CO_2 [17, 18] and O_2 [18] in NaCl brine. However, a brief description of this technique will be presented (for more details, see Chabab et al. [17, 18]).

The technique based on the "static-analytic" method is illustrated in Figure 2 and consists of:

1- Performing the Equilibrium in a Cell (EC) placed in an Oven (O) to control the temperature, and equipped with a Variable Speed Stirrer (VSS), pressure and temperature sensors, and ROLSI® (Rapid On-Line Sampler-Injector, French patent number 0304073) capillary samplers.

The desired pressure is less controlled than the temperature, and is obtained by adding through a manual valve (V1) the necessary quantity of gas to the saline solution previously loaded in the cell.

2- Taking a sample from the liquid phase by the ROLSI® and transferring it to the analytical part once the thermodynamic equilibrium (temperature and pressure stabilization) has been reached.

3- Quantification of non-electrolyte compounds (H_2 and H_2O) by GC analysis.

This last step depends on GC detector calibration, which is carried out under the same measurement conditions, to convert the areas obtained by integration of the chromatogram peaks into numbers of moles. Using the mole number of H_2 (n_{H_2}) and H_2O (n_{H_2O}), the solubility of H_2 in the saline solution in terms of "salt-free" mole fraction x_{H_2} is determined:

$$x_{H_2} = \frac{n_{H_2}}{n_{H_2} + n_{H_2O}} \quad \textbf{(1)}$$

The solubility in terms of "salt-free" mole fraction x_{H_2} can be converted in terms of molality m_{H_2} (in mol/kgw) easily by the following relationship:

$$m_{H_2} = \frac{1000\, x_{H_2}}{M_{H_2O}(1 - x_{H_2})} \quad \textbf{(2)}$$

or in terms of "true" mole fraction by

$$x_{H_2}^{true} = \frac{n_{H_2}}{n_{H_2} + n_{H_2O} + n_s} = \frac{n_{H_2}}{n_{H_2} + n_{H_2O} + m_s n_{H_2O} M_{H_2O}} = \frac{x_{H_2}}{x_{H_2} + \left(1 - x_{H_2}\right)\left(1 + m_s M_{H_2O}\right)} \quad \textbf{(3)}$$

where n_s and m_s are respectively the mole number and molality (in mol/kgw) of the salt (NaCl), and M_{H_2O} is the molecular weight of water (in g/mol).

To check repeatability and to obtain data that are more representative of the real solubility, the procedure described above is repeated several times.

2.4. Experimental results

Experimental measurements of H_2 solubility in H_2O+NaCl were carried out at temperatures between 323 K and 373 K, at pressures up to 230 bar and at NaCl molalities (m=mol/kgw) equal to 0 (pure water), 1m, 3m and 5m. These measurements are presented in Table 4, knowing that the reported data (P, T, x_{H_2}) with the associated uncertainties are an average of several repeated measurements. The method proposed by NIST [54] was used to estimate measurement uncertainties. The uncertainties related to the TCD calibration (determination of mole numbers) and repeatability, are taken into account in the calculation of the total uncertainty on composition $u(x_{H_2})$, by the following relationship:

$$u(x_{H_2}) = \pm\sqrt{u^2_{calibration}(x_{H_2}) + u^2_{repeatability}(x_{H_2})} \quad \textbf{(4)}$$

Since the composition x_{H_2} is determined from the values of the other independent measurands (number of moles of the compounds: n_{H_2} and n_{H_2O}), the law of propagation of uncertainty should apply [55-58]:

$$u(x_{H_2}) = \pm\sqrt{\left(\frac{\partial x_{H_2}}{\partial n_{H_2}}\right)^2 u^2(n_{H_2}) + \left(\frac{\partial x_{H_2}}{\partial n_{H_2O}}\right)^2 u^2(n_{H_2O}) + u^2_{repeatability}(x_{H_2})}$$
$$= \pm\sqrt{\left(\frac{1 - x_{H_2}}{n_{H_2} + n_{H_2O}}\right)^2 u^2(n_{H_2}) + \left(\frac{x_{H_2}}{n_{H_2} + n_{H_2O}}\right)^2 u^2(n_{H_2O}) + u^2_{repeatability}(x_{H_2})} \quad \textbf{(5)}$$

The uncertainty $u(n_i)$ involved in the calculation of the mole number n_i takes into account the injection of the constituents by the syringe (for GC calibration) $u_{inj}(n_i)$ and the polynomial equation $u_{pol.eq}(n_i)$ relating the surface area S (obtained by integration of the chromatogram) and the mole number n:

$$u(n_i) = \sqrt{u^2_{inj}(n_i) + u^2_{pol.eq}(n_i)} \quad \textbf{(6)}$$

The calculation of $u_{repeatability}(x)$, $u_{inj}(n_i)$ and $u_{pol.eq}(n_i)$ are described in detail by Soo [56], Zhang [57] and El Abbadi [58]. In the same way repeatability and calibration (polynomial equation) are the two sources of error on the measurement of pressure $u(P)$ and temperature $u(T)$ uncertainties.

Since the water content in the H_2-rich phase is very low, and considering the vapor phase as ideal, the Krichevsky-Kasarnovsky [59] equation $\left(ln\left(\frac{f_g}{x_g}\right) = ln(K_H) + PF = f(P)\right)$ derived from the gamma-phi approach is reduced to: $\left(ln\left(\frac{P}{x_g}\right) = f(P)\right)$, where f_g, x_g and K_H are respectively the fugacity, the mole fraction and the Henry constant of the gas, PF is the Poynting Factor and $f(P)$ is a linear function with respect to the pressure P.

In Figure 3, the measured data were plotted as $ln\left(\frac{P}{x_{H_2}}\right) = f(P)$ to check their linearity. By comparing with the predictions of the e-PR-CPA model (see next section), in general, one can observe a good linearity even by neglecting the fugacity coefficient and water content. Only a few points at low pressure are slightly shifted, this is due to the fact that the water content is not negligible at low pressure and also to the experimental protocol. The H_2 solubility in pure water was measured to validate the calibration by comparing with literature data. Figure 3 shows that the obtained measurements are in good agreement with the literature data.

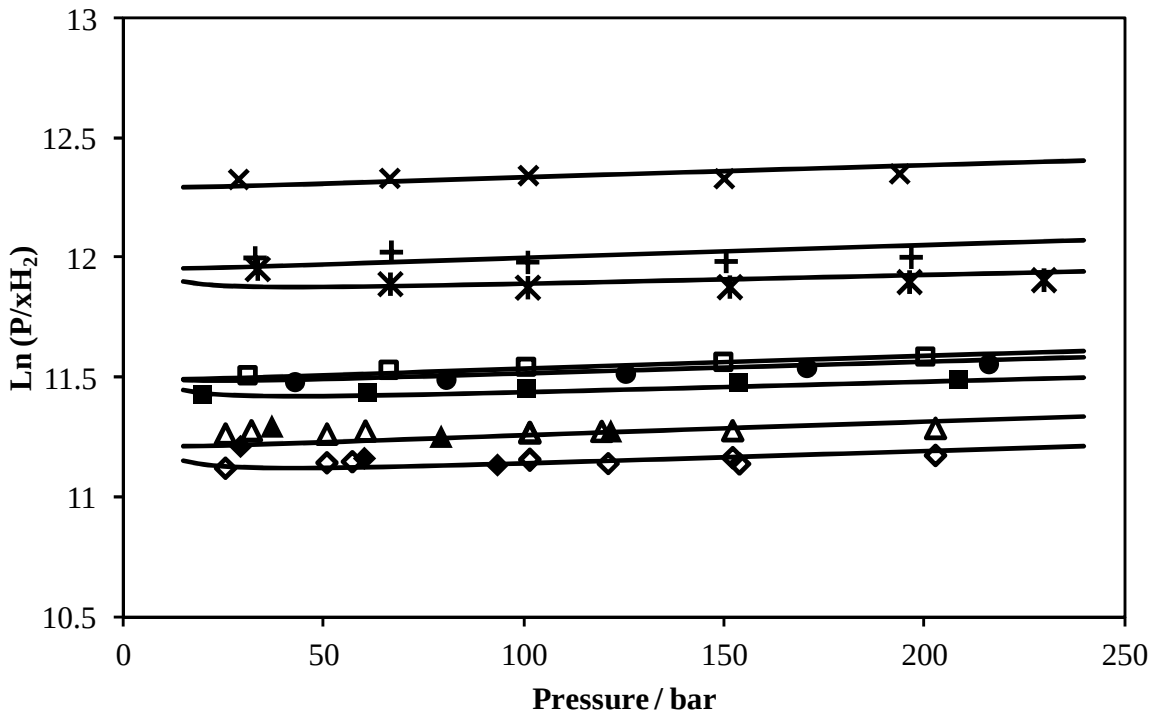

Figure 3: Solubility of H_2 in H_2O ± NaCl. Literature data [20, 49, 52] are represented by black symbols (△: 323 K – pure water; ◊: 373K – pure water) and measured ones (Table 4) are represented by colored symbols (▲: 323 K – pure water; □: 323 K – 1m; +: 323 K – 3m; ×: 323 K – 5m; ●: 348 K – 1m; ◆: 373K – pure water; ■: 373 K – 1m; ✱: 373 K – 3m). The solid lines represent the predictions of the e-PR-CPA model.

Table 4: Measured solubility of H_2 in the H_2O + NaCl solutions, expressed as "salt-free" mole fractions (Eq. (1)). $u(T) = 0.02\ K$ and $u(P) = 5\ kPa$.

m_{NaCl} (mol/kg_w)	T (K)	P (bar)	x_{H_2}	$u(x_{H_2})$
0	323.18	37.108	0.000461	2.0E-05
	323.18	79.366	0.001030	3.0E-05
	323.19	121.706	0.001544	4.0E-05
	372.71	29.272	0.000396	2.5E-05
	372.73	60.213	0.000857	3.5E-05
	372.72	93.426	0.001368	6.0E-05
1	323.20	30.828	0.000309	1.0E-05
	323.21	66.068	0.000648	2.0E-05
	323.21	100.354	0.000972	3.5E-05
	323.21	149.657	0.001419	4.0E-05
	323.21	200.093	0.001855	6.0E-05
	347.90	42.907	0.000444	1.0E-05
	347.91	80.673	0.000827	2.0E-05
	347.90	125.504	0.001255	4.0E-05
	347.90	170.730	0.001667	4.5E-05
	347.91	216.205	0.002076	6.0E-05
	372.73	19.884	0.000217	1.0E-05
	372.76	60.987	0.000659	2.0E-05
	372.76	100.677	0.001071	3.5E-05
	372.78	153.553	0.001595	4.5E-05
	372.72	208.620	0.002132	7.0E-05
3	323.20	32.736	0.000201	1.5E-05
	323.18	66.733	0.000400	2.0E-05
	323.20	100.832	0.000631	2.0E-05
	323.21	150.342	0.000938	3.5E-05
	323.20	196.595	0.001204	4.0E-05
	372.75	33.387	0.000215	1.5E-05
	372.74	66.536	0.000456	1.5E-05
	372.74	100.855	0.000702	3.0E-05
	372.76	151.296	0.001050	4.0E-05
	372.75	196.178	0.001333	4.0E-05
	372.76	229.720	0.001549	5.0E-05
5	323.19	28.623	0.000127	5.0E-06
	323.19	66.385	0.000293	1.0E-05

323.19	100.979	0.000440	1.0E-05
323.20	149.900	0.000662	2.0E-05
323.19	193.702	0.000838	3.5E-05

3. Thermodynamic modeling

Asymmetric and symmetric thermodynamic approaches were used for modeling liquid-vapor equilibria of the binary H_2+H_2O and ternary H_2+H_2O+NaCl.

3.1. Approaches and models

In the asymmetric approach, the non-ideality of the vapor phase is taken into account by considering fugacity coefficients in the vapor phase, which are obtained by using an equation of state. However the non-ideality of the liquid phase is considered with a G-excess model through the activity coefficients. Based on this approach, the **Geochemical model** implemented in CHESS/HYTEC software and proposed by Corvisier [60, 61] was tested.

In the symmetric approach, the two phases (liquid and vapor) in equilibrium are represented by the same model (Equation of State (EoS)). Based on this approach, two equations of state (**SW** and **e-PR-CPA**) were tested.

These three models (Geochemical, SW, and e-PR-CPA models) were presented in details in our previous work [17, 18], however a brief description of the models and their parameters resulting from this work are given hereafter.

A. Geochemical model

This model solves a large set of mass balances and mass action laws to calculate the whole system speciation (i.e. aqueous, gaseous and solid quantities and activities/fugacities). Nevertheless, to handle multi-components either for the gas phase and the electrolyte, equations shall remain generic. For the gas phase, the PR-SW EoS is used with the classical mixing rule. For the aqueous solution and particularly for saline solutions with high ionic strength, activity coefficients are calculated using Specific Ion Theory (SIT) showing satisfactory results.

Simulations presented here are run along with the Thermoddem database including parameters for PR-SW EoS (Blanc et al. [62]) with the addition of the Henry's constant for H_2 (Harvey [63]), and parameters for molar volume of the dissolved gaseous component at infinite dilution

(Shock et al. [64]). Gas binary interaction parameters for PR-SW and aqueous binary interactions parameters for SIT have been fitted on experimental data.

- $k_{H_2H_2O}$ is equal to 0.445.
- $\varepsilon_{H^+Cl^-}$ and $\varepsilon_{Na^+Cl^-}$ are equal to -0.097 and -0.035 using HCl and NaCl solutions activity measurements (Schneider et al. [65], Sakaida and Kakiuchi [66]; Khoshkbarchi and Vera [67]).
- $\varepsilon_{H_2Na^+}$ vary with temperature (from 0.090 at 25°C to 0.108 at 100°C) using H_2 solubility measurements in NaCl solutions.

B. Soreide and Whitson (SW) EoS

The Soreide and Whitson [16] EoS is widely used in oil and gas applications especially for gas/water/salt systems, and is available in several thermophysical calculators and reservoir simulators. This EoS does not consider the salt (NaCl) as a compound, but takes into account its presence by adding a dependence of the model parameters (water alpha function $\alpha_w(T)$ and the aqueous phase binary interaction parameter k_{ij}^{AQ}) to the NaCl molality. The use of two binary interaction parameters (k_{ij}^{AQ} for the aqueous phase and k_{ij}^{NA} for the non-aqueous phase) makes the model inconsistent (similar to an asymmetric approach) and very empirical (to be used just within the range of parameter fit). Concerning $k_{H_2-H_2O}^{AQ}$ and $k_{H_2-H_2O}^{NA}$, we have taken the expression recently proposed by Lopez-Lazaro et al. [13] which performs well when compared with our new data and readjusted its coefficients on H_2 solubility data in brine (including those obtained in this work) and on water content data.

$$\left(k_{H_2-H_2O}\right)_{SW} = A_0\left(1+\alpha_0 {m_{NaCl}}^{\beta_0}\right) + A_1\frac{T}{T_{c,H_2}}\left(1+\alpha_1 {m_{NaCl}}^{\beta_1}\right) + A_2\exp\left(A_3\frac{T}{T_{c,H_2}}\right) \quad \textbf{(7)}$$

The coefficients A_x, α_x and β_x given by Lopez-Lazaro et al. [13] and those proposed in this work are listed in Table 5. The H_2 critical temperature $T_{c,H_2} = 33.145\,K$ was taken from REFPROP 10.0 [68]. The readjustment of the coefficients has led to a significant improvement (comparing with the coefficients given by Lopez-Lazaro et al.) in the estimation of the solubility of H_2 in water and NaCl-brine (AAD of 2.6% instead of 4.3%), and of the water content in the H_2-rich phase (AAD of 2.5% instead of 6.6%).

Table 5: Optimized coefficients of the binary interaction parameters in aqueous $k^{AQ}_{H_2-H_2O}$ and non-aqueous $k^{NA}_{H_2-H_2O}$ phases (Equation 7).

		Lopez-Lazaro et al. [13]		This work	
		$k^{AQ}_{H_2-H_2O}$	$k^{NA}_{H_2-H_2O}$	$k^{AQ}_{H_2-H_2O}$	$k^{NA}_{H_2-H_2O}$
A_0		-2.513	2.5	-2.34	-0.3776
A_1		0.181	-0.179	0.166	0.08385
A_2		-12.723	-	-12.69	-
A_3		-0.499	-	-0.474	-
α_0		6.8×10^{-4}	-	3.88×10^{-3}	-
α_1		0.038	-	0.049	-
β_0		0.443	-	0.443	-
β_1		0.799	-	0.799	-
AAD (%)	x_{H_2}	4.3		2.6	
	y_{H_2O}	6.6		2.5	

C. e-PR-CPA EoS

Unlike the SW EoS, the e-PR-CPA (electrolyte Peng-Robinson Cubic Plus Association) EoS takes into account the presence of salt theoretically. This model considers molecular interactions (attraction, dispersion, and association) by the PR (Peng-Robinson) cubic term [69] and the Wertheim's association theory [70], and ionic interactions ion/ion by the MSA (Mean Spherical Approximation) theory [71] and ion/solvent (solvation phenomenon) by the Born term [72]. The expression of the residual Helmholtz free energy of the e-PR-CPA EoS is as follows:

$$\frac{A^{res}_{e-PR-CPA}}{RT} = \frac{A^{PR}}{RT} + \frac{A^{Association}}{RT} + \frac{A^{MSA}}{RT} + \frac{A^{Born}}{RT} \quad \textbf{(8)}$$

The expression of the residual Helmholtz energy A^{res} is the key function in equilibrium thermodynamics, because all other thermodynamic properties (pressure, fugacity coefficient, enthalpy, etc.) are calculable from the partial derivatives of A^{res} with respect to temperature, volume, and mole number. Further details on the different terms of Equation 8 and their calculation methods as well as the model parameterization (for pure H_2O and H_2O+NaCl) are presented in our previous paper [17].

Since H_2 is not considered as an associative species, the solvation (cross-association interaction) of H_2 by H_2O molecules was not considered (no Lewis Acid − Lewis Base interaction). Only the binary interaction parameters (of the cubic term PR) of the $H_2 - H_2O$, $H_2 - Na^+$, and $H_2 - Cl^-$ pairs were considered in the fit. Temperature dependence was considered in the $H_2 - H_2O$ interaction, and salt concentration dependence was considered in the $H_2 -$ ion interactions.

$$k_{H_2-H_2O} = -2.51 \times 10^{-5}\, T^2 + 2.24 \times 10^{-2}\, T - 4.44 \quad \textbf{(9)}$$

$$k_{H_2-Na^+} = -1.58\, m_{NaCl} - 5.7 \quad \textbf{(10)}$$

$$k_{H_2-Cl^-} = 0.96\, m_{NaCl} + 4.87 \quad \textbf{(11)}$$

3.2. H_2+H_2O system :H_2 solubility and water content

The models presented above were used to process data of H_2 solubility in pure water. In Figure 4, literature data and "validation" measurements are presented together with calculated solubilities at 323 and 373 K. Compared to experimental data, all three models estimate accurately the solubility of H_2 in pure water at different temperatures and pressures. The solubility is higher at 373 K, this can be better visualized by studying the effect of temperature on the solubility. In Figure 5, isobaric solubility data smoothed by IUPAC [20] (with an accuracy of ± 1 or 2%) between 51 and 203 bar are compared with model predictions. The models reproduce very well the effect of temperature on solubility at different fixed pressures, and estimate well the minimum solubility temperature which is close to 329 (± 2) K.

The prediction of water content in the H_2-rich phase by the developed models was also investigated. Gillespie and Wilson [48] data were used in the adjustment of the SW EoS and geochemical model. However, for the e-PR-CPA model, it is not necessary to include them in the parameter fitting for a good representation of the vapor phase. With a zero binary interaction parameter ($k_{H_2-H_2O} = 0$), the e-PR-CPA model reproduces the Gillespie and Wilson [48] data with an Average Absolute Deviation (AAD) of 3.1% over a wide range of temperature (311 − 478 K) and pressure (3 − 138 bar), whereas with a non-zero $k_{H_2-H_2O}$ (Equation 9), the model reproduces the same water content data with an AAD of 2.8%. The calculation of water content with CPA-type models is not very sensitive to variations in binary interaction parameters, which was also observed by Hajiw et al. [73] using the GC-PR-CPA model. This is a great advantage

of CPA-type models, as only gas solubility data are needed to parameterize the model and hence predict water content.

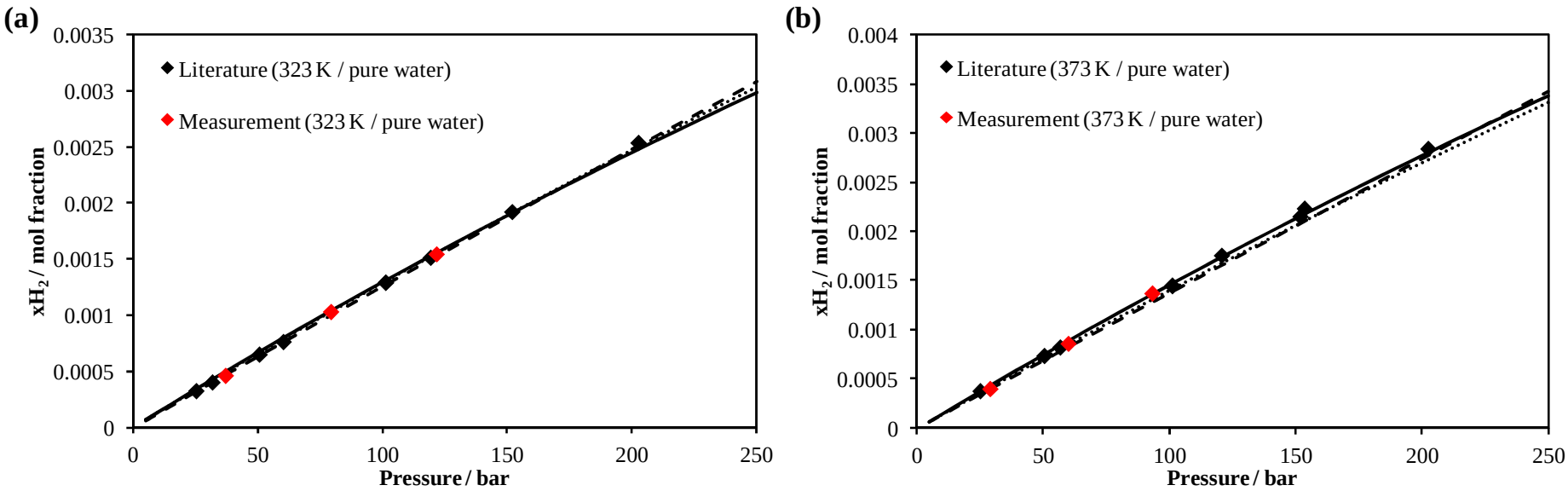

Figure 4 : Solubility of H_2 in H_2O at 323 K (a) and 373 K (b). Literature data [20, 49, 52] are represented by black symbols (◆) and measured ones (Table 4) are represented by red symbols (◆). The solid, dotted and dashed lines represent the H_2 solubilities calculated by the e-PR-CPA, SW, and geochemical models, respectively.

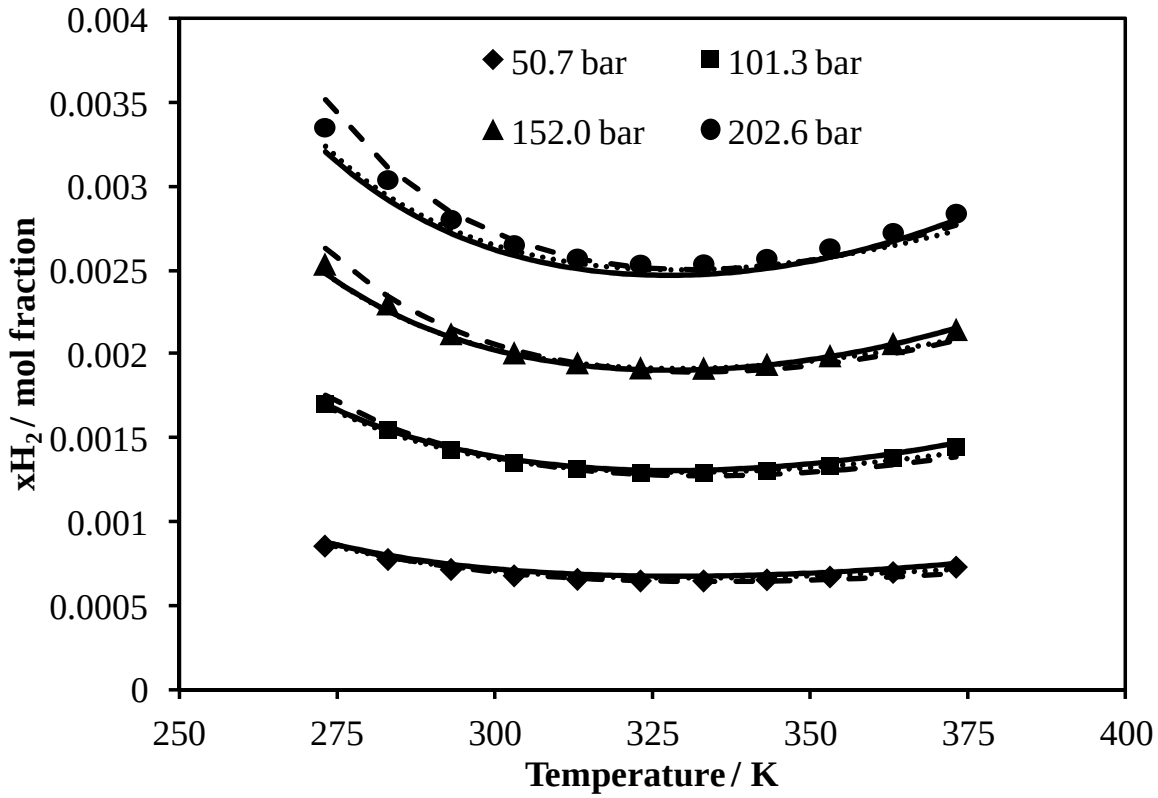

Figure 5 : Isobars of solubility of H_2 in H_2O showing solubility minimum temperatures at 50, 100, 150 and 200 atm. Comparison of data smoothed by IUPAC [20] represented by black symbols, with predictions by e-PR-CPA, SW, and geochemical models represented by solid, dotted, and dashed lines, respectively.

In Figure 6, one can show that all models are able to predict the water contents, although only H_2 solubility data were used to determine the e-PR-CPA model interaction parameters. All three models can be used to generate data with high accuracy especially in the parameter fitting range, however due to its theoretical background, the e-PR-CPA model can be used with a high level of confidence for the prediction of water content outside the parameter fitting range. In Table 6, predictions of water content in the H_2+H_2O binary system are generated with the e-PR-CPA model at different temperatures and pressures.

Table 6 : H_2+H_2O binary system: Predicted water content y_{H_2O} in H_2-rich phase by the e-PR-CPA model.

P (bar)	T (K)					
	298.15	323.15	348.15	373.15	398.15	423.15
2	0.01607391	0.06204187	0.19388235	0.50968425		
3	0.01073722	0.04142540	0.12952971	0.34180465	0.77743831	
4	0.00806878	0.03111404	0.09729662	0.25720417	0.58886005	
5	0.00646768	0.02492622	0.07793854	0.20623041	0.47400614	
6	0.00540027	0.02080058	0.06502553	0.17215844	0.39671208	0.80424530
7	0.00463784	0.01785348	0.05579820	0.14777733	0.34114267	0.69524713
8	0.00406600	0.01564304	0.04887564	0.12946735	0.29926734	0.61233208
9	0.00362125	0.01392374	0.04349020	0.11521191	0.26657938	0.54713811
10	0.00326544	0.01254825	0.03918107	0.10379850	0.24035410	0.49453249
11	0.00297432	0.01142282	0.03565489	0.09445423	0.21884731	0.45119016
12	0.00273173	0.01048494	0.03271605	0.08666320	0.20089066	0.41486231
13	0.00252646	0.00969133	0.03022907	0.08006782	0.18567212	0.38397358
14	0.00235051	0.00901108	0.02809719	0.07441248	0.17260976	0.35738747
15	0.00219802	0.00842151	0.02624940	0.06950956	0.16127564	0.33426351
16	0.00206459	0.00790564	0.02463248	0.06521826	0.15134806	0.31396673
17	0.00194687	0.00745045	0.02320569	0.06143086	0.14258047	0.29600849
18	0.00184222	0.00704583	0.02193736	0.05806350	0.13478078	0.28000665
19	0.00174859	0.00668379	0.02080247	0.05504999	0.12779709	0.26565799
20	0.00166432	0.00635795	0.01978103	0.05233732	0.12150770	0.25271891
21	0.00158808	0.00606315	0.01885682	0.04988260	0.11581397	0.24099140
22	0.00151877	0.00579513	0.01801659	0.04765068	0.11063510	0.23031289
23	0.00145548	0.00555042	0.01724940	0.04561256	0.10590427	0.22054866
24	0.00139747	0.00532610	0.01654611	0.04374403	0.10156574	0.21158609
25	0.00134410	0.00511972	0.01589906	0.04202478	0.09757266	0.20333035
26	0.00129484	0.00492922	0.01530176	0.04043759	0.09388534	0.19570098
27	0.00124923	0.00475282	0.01474868	0.03896782	0.09046995	0.18862930
28	0.00120687	0.00458902	0.01423510	0.03760290	0.08729748	0.18205630
29	0.00116744	0.00443651	0.01375692	0.03633199	0.08434290	0.17593104
30	0.00113063	0.00429417	0.01331060	0.03514570	0.08158451	0.17020926
35	0.00097815	0.00370444	0.01146140	0.03022994	0.07014866	0.14645440
40	0.00086380	0.00326211	0.01007428	0.02654184	0.06156294	0.12858457
45	0.00077486	0.00291803	0.00899524	0.02367247	0.05487974	0.11465357
50	0.00070370	0.00264273	0.00813187	0.02137636	0.04952962	0.10348815
55	0.00064549	0.00241746	0.00742536	0.01949726	0.04514979	0.09433894
60	0.00059697	0.00222971	0.00683650	0.01793097	0.04149814	0.08670488
65	0.00055592	0.00207081	0.00633813	0.01660535	0.03840692	0.08023824
70	0.00052074	0.00193459	0.00591088	0.01546884	0.03575625	0.07469013
75	0.00049024	0.00181651	0.00554051	0.01448363	0.03345816	0.06987772
80	0.00046355	0.00171317	0.00521637	0.01362138	0.03144663	0.06566369
85	0.00044001	0.00162196	0.00493029	0.01286039	0.02967116	0.06194288

90	0.00041907	0.00154087	0.00467594	0.01218379	0.02809247	0.05863342
95	0.00040034	0.00146829	0.00444830	0.01157827	0.02667951	0.05567060
100	0.00038348	0.00140295	0.00424336	0.01103315	0.02540747	0.05300262
105	0.00036822	0.00134382	0.00405789	0.01053982	0.02425623	0.05058751
110	0.00035435	0.00129005	0.00388923	0.01009122	0.02320934	0.04839089
115	0.00034168	0.00124094	0.00373519	0.00968152	0.02225320	0.04638436
120	0.00033007	0.00119590	0.00359394	0.00930585	0.02137649	0.04454424
125	0.00031938	0.00115445	0.00346394	0.00896013	0.02056967	0.04285060
130	0.00030951	0.00111617	0.00334390	0.00864092	0.01982470	0.04128660
135	0.00030037	0.00108072	0.00323271	0.00834525	0.01913471	0.03983787
140	0.00029189	0.00104778	0.00312943	0.00807062	0.01849381	0.03849209
145	0.00028398	0.00101710	0.00303323	0.00781484	0.01789694	0.03723865
150	0.00027660	0.00098846	0.00294340	0.00757604	0.01733968	0.03606834
155	0.00026969	0.00096165	0.00285934	0.00735257	0.01681822	0.03497312
160	0.00026322	0.00093650	0.00278049	0.00714299	0.01632920	0.03394598
165	0.00025713	0.00091286	0.00270639	0.00694604	0.01586967	0.03298074
170	0.00025140	0.00089060	0.00263662	0.00676061	0.01543703	0.03207196
175	0.00024599	0.00086961	0.00257080	0.00658571	0.01502899	0.03121481
180	0.00024088	0.00084976	0.00250861	0.00642046	0.01464349	0.03040498
185	0.00023605	0.00083098	0.00244975	0.00626409	0.01427871	0.02963867
190	0.00023146	0.00081318	0.00239396	0.00611589	0.01393301	0.02891243
195	0.00022711	0.00079628	0.00234101	0.00597523	0.01360493	0.02822319
200	0.00022298	0.00078021	0.00229068	0.00584155	0.01329315	0.02756819

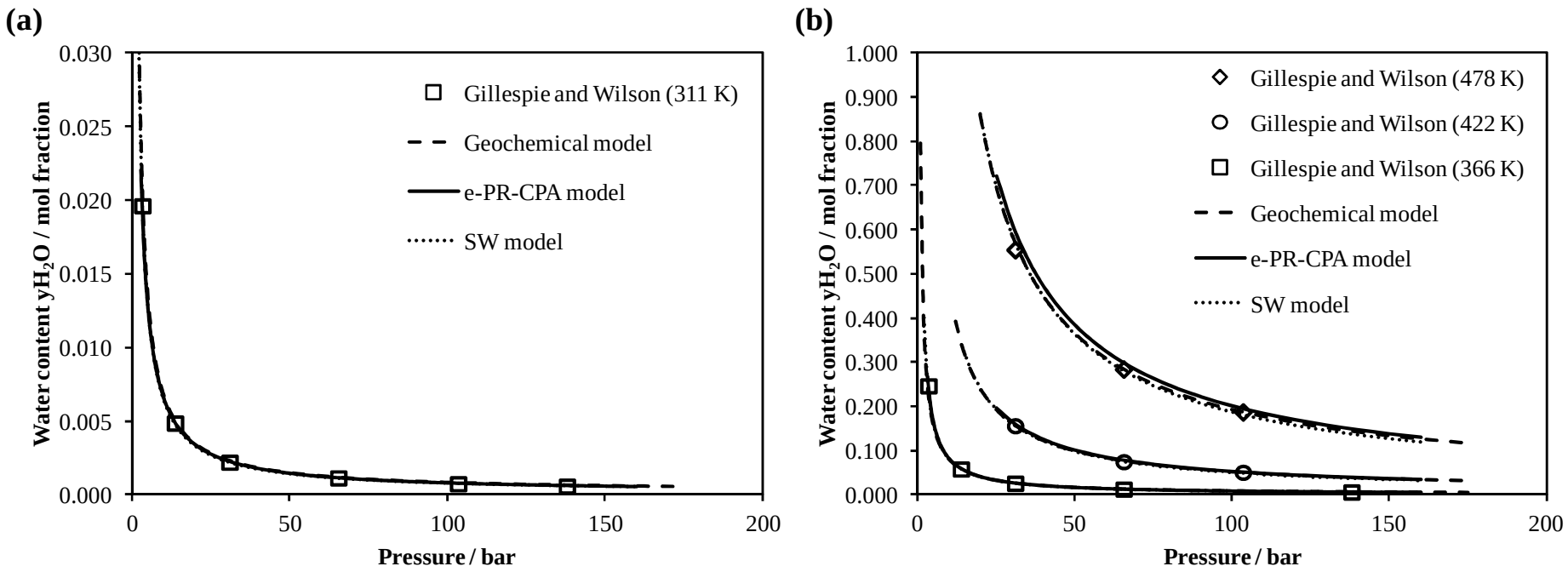

Figure 6 : Water content in H_2-rich phase at (a): 311 K; (b): 366, 422, and 478 K. Comparison of literature data [48] represented by black symbols, with predictions with the e-PR-CPA, SW, and geochemical models represented by solid, dotted, and dashed lines, respectively.

3.3. H_2+H_2O+NaCl system: H_2 solubility

As with all gases, the presence of salt in water is expected to decrease the solubility of hydrogen (salting-out effect) in a manner proportional to the concentration of the salt until the solution is saturated. Both atmospheric pressure data of H_2 solubilities in H_2O+NaCl from literature as well as new high pressure data measured in this work were included in the parameterization of the models (Geochemical, SW, and e-PR-CPA). The modeling results are shown in Figure 7. The three models correlate solubility data at different temperatures (323−373 K) and pressures (up to 230 bar) with high accuracy and capture accurately the salting-out effect over a wide range of NaCl concentration (from salt-free solution to highly concentrated brine).

Given its very good performance and predictive capability, the e-PR-CPA model was used to predict solubility minimum temperatures in the presence of NaCl. In Figure 8.a, isothermal data (at 323, 348 and 373 K) of the solubility of H_2 in water and brine (1m NaCl) as a function of pressure are presented and compared with the model calculations. In Figure 8.b, the prediction of the evolution of H_2 solubility as function of temperature at 152 bar (which is a pressure more or less representative of hydrogen geological storage conditions) is compared with salt-free data and measured data around 152 bar. Since the calculated solubilities are in very good agreement with the IUPAC (in pure water) and measured (in brine) data, accurate H_2 solubility values in water and brine were generated at different temperatures, pressures and NaCl molalities with the e-PR-CPA model and listed in Table 8.

Correlation for H_2 solubility in water and NaCl-brine:

For quick calculations of the solubility of H_2 in water and brine, a simple correlation taking into account the effect of temperature, pressure and molality has been developed. The proposed correlation is based on a Setschenow-type relationship, and is defined by:

$$ln\left(\frac{x_{H_2}}{x^0_{H_2}}\right) = a_1 m^2_{NaCl} + a_2 m_{NaCl} \quad \textbf{(12)}$$

Knowing the solubility $x^0_{H_2}$ of H_2 in pure water at system temperature and pressure, the solubility x_{H_2} of H_2 in brine at a molality m_{NaCl} is therefore easily obtained by Equation 12. The solubility data (from IUPAC) of H_2 in pure water were correlated by the following equation:

$$x_{H_2}^0 = b_1 PT + \frac{b_2 P}{T} + b_3 P + b_4 P^2 \quad \textbf{(13)}$$

In Equation 13, the temperature T is in K and the pressure P is in bar. The coefficients a_i and b_i in Equations 12 and 13 are listed in Table 7.

Table 7: Coefficients for Equations 12 and 13.

a_1	a_2	b_1	b_2	b_3	b_4
0.018519	-0.30185103	3.338844×10^{-7}	0.0363161	-0.00020734	$-2.1301815 \times 10^{-9}$

The correlation for solubility in brine (Equation 12) is reduced to the correlation for solubility in pure water (Equation 13) when the molality is equal to 0.

When compared with IUPAC and measured data, the two correlations developed are capable of estimating the solubility in pure water and brine with high precision (see Figure 9) with an AAD of 0.5% and 2% respectively, and an overall AAD of 1%. However, it is recommended to use the two correlations only in the range of their coefficients adjustments, which are:

- For H_2 solubility in pure water (Equation 13): 273.15 < T (K) < 373.15; 1 < P (bar) < 203
- For H_2 solubility in NaCl-brine (Equation 12): 323.15 < T (K) < 373.15; 10 < P (bar) < 230; 0 < molality (mol/kgw) < 5

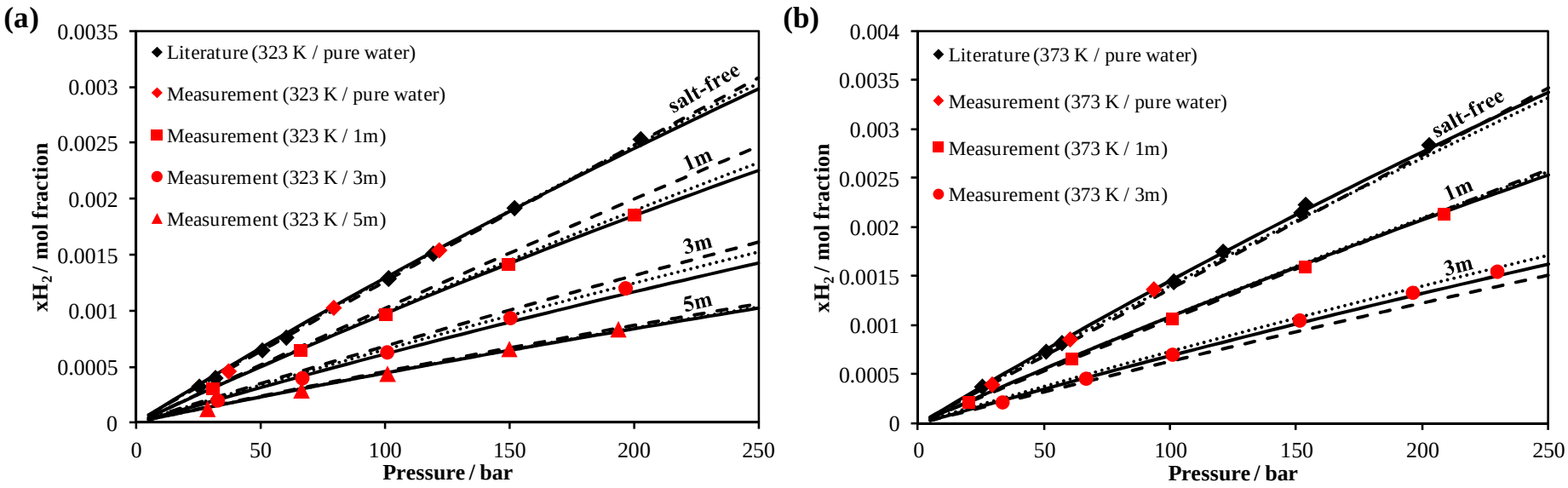

Figure 7 : Solubility of H_2 in H_2O + NaCl at 323 K (a) and 373 K (b) and different NaCl molalities. Literature data [20, 49, 52] are represented by black symbols and measured ones (Table 4) are represented by red symbols. The solid, dotted and dashed lines represent the H_2 solubilities calculated by the e-PR-CPA, SW, and geochemical models, respectively.

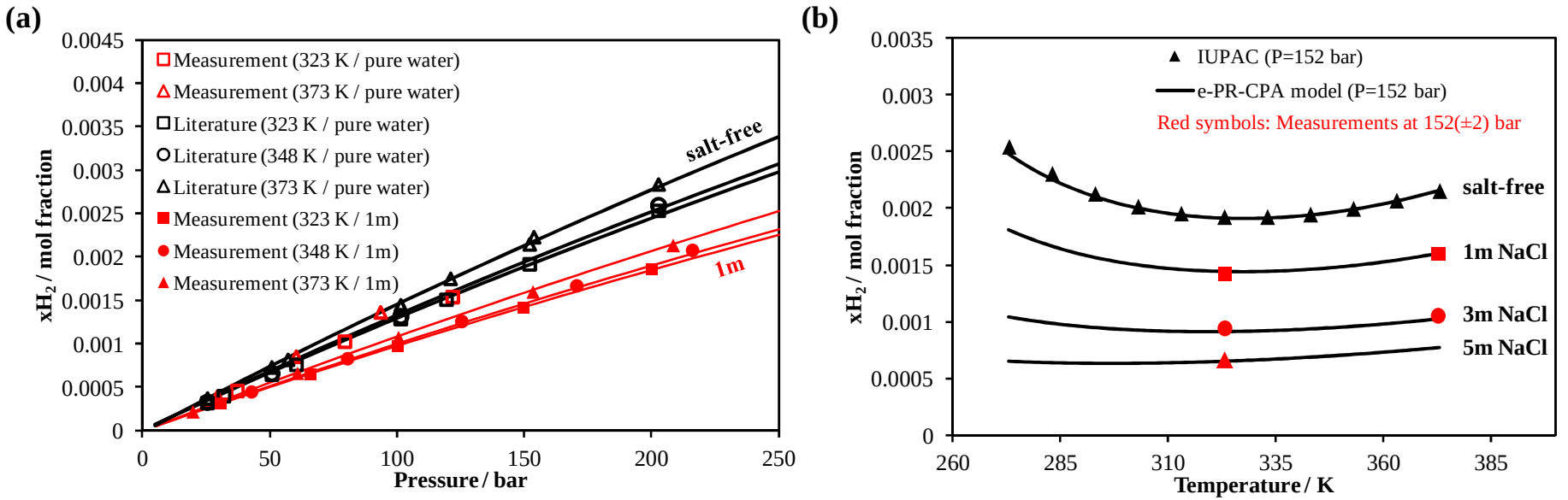

Figure 8 : Effect of temperature, pressure and NaCl concentration (molality) on H_2 solubility. Comparison of literature [20, 49, 52] and some measured (Table 4) data with e-PR-CPA model predictions.

Table 8 : Calculated solubility (in terms of salt-free mole fraction) of H_2 in water ± NaCl by the e-PR-CPA model.

T (K)	P (bar)										
	5	10	15	20	25	50	75	100	200	300	400
m = 0 mol/kgw											
298.15	0.0000732	0.0001463	0.0002190	0.0002911	0.0003628	0.0007144	0.0010550	0.0013854	0.0026164	0.0037247	0.0047326
323.15	0.0000669	0.0001351	0.0002029	0.0002702	0.0003371	0.0006654	0.0009839	0.0012932	0.0024473	0.0034877	0.0044335
348.15	0.0000649	0.0001348	0.0002043	0.0002733	0.0003419	0.0006789	0.0010062	0.0013242	0.0025127	0.0035852	0.0045602
373.15	0.0000619	0.0001390	0.0002155	0.0002917	0.0003674	0.0007393	0.0011007	0.0014522	0.0027674	0.0039554	0.0050353
398.15	0.0000487	0.0001385	0.0002279	0.0003168	0.0004051	0.0008395	0.0012618	0.0016728	0.0032122	0.0046038	0.0058690
423.15		0.0001151	0.0002242	0.0003326	0.0004405	0.0009709	0.0014870	0.0019894	0.0038732	0.0055776	0.0071276
m = 1 mol/kgw											
298.15	0.0000549	0.0001097	0.0001642	0.0002183	0.0002721	0.0005357	0.0007910	0.0010387	0.0019614	0.0027920	0.0035470
323.15	0.0000506	0.0001021	0.0001533	0.0002041	0.0002547	0.0005028	0.0007436	0.0009776	0.0018525	0.0026432	0.0033638
348.15	0.0000491	0.0001017	0.0001539	0.0002058	0.0002575	0.0005112	0.0007580	0.0009981	0.0018988	0.0027159	0.0034625
373.15	0.0000467	0.0001038	0.0001606	0.0002171	0.0002732	0.0005495	0.0008186	0.0010808	0.0020672	0.0029654	0.0037883
398.15	0.0000374	0.0001024	0.0001671	0.0002315	0.0002955	0.0006109	0.0009184	0.0012185	0.0023505	0.0033852	0.0043359
423.15	0.0000091	0.0000858	0.0001622	0.0002382	0.0003139	0.0006867	0.0010508	0.0014066	0.0027525	0.0039874	0.0051257
m = 3 mol/kgw											
298.15	0.0000334	0.0000668	0.0001000	0.0001330	0.0001657	0.0003263	0.0004820	0.0006330	0.0011965	0.0017049	0.0021678
323.15	0.0000319	0.0000642	0.0000964	0.0001284	0.0001601	0.0003163	0.0004682	0.0006159	0.0011703	0.0016741	0.0021357
348.15	0.0000314	0.0000648	0.0000980	0.0001310	0.0001639	0.0003256	0.0004832	0.0006369	0.0012166	0.0017472	0.0022360
373.15	0.0000301	0.0000662	0.0001021	0.0001379	0.0001735	0.0003489	0.0005203	0.0006877	0.0013222	0.0019067	0.0024480
398.15	0.0000245	0.0000650	0.0001053	0.0001454	0.0001853	0.0003824	0.0005753	0.0007641	0.0014827	0.0021486	0.0027686
423.15	0.0000082	0.0000548	0.0001012	0.0001474	0.0001934	0.0004206	0.0006435	0.0008621	0.0016970	0.0024751	0.0032033
m = 5 mol/kgw											
298.15	0.0000227	0.0000453	0.0000678	0.00009019	0.00011241	0.0002214	0.0003271	0.0004298	0.0008131	0.0011596	0.0014756
323.15	0.0000227	0.0000458	0.0000688	0.00009163	0.00011433	0.0002260	0.0003346	0.0004404	0.0008383	0.0012013	0.00153497
348.15	0.0000231	0.00004764	0.00007209	0.00009642	0.00012063	0.0002399	0.0003562	0.00046986	0.0008998	0.00129521	0.00166131
373.15	0.0000223	0.00004934	0.00007623	0.000103	0.00012964	0.0002611	0.0003897	0.00051558	0.00099429	0.0014379	0.0018512
398.15	0.00001797	0.0000484	0.0000787	0.00010888	0.00013893	0.0002874	0.00043296	0.00057574	0.0011212	0.00163005	0.00210691
423.15	0.00000496	0.00003989	0.0000747	0.00010937	0.00014392	0.00031479	0.00048262	0.00064754	0.00128025	0.00187407	0.00243355

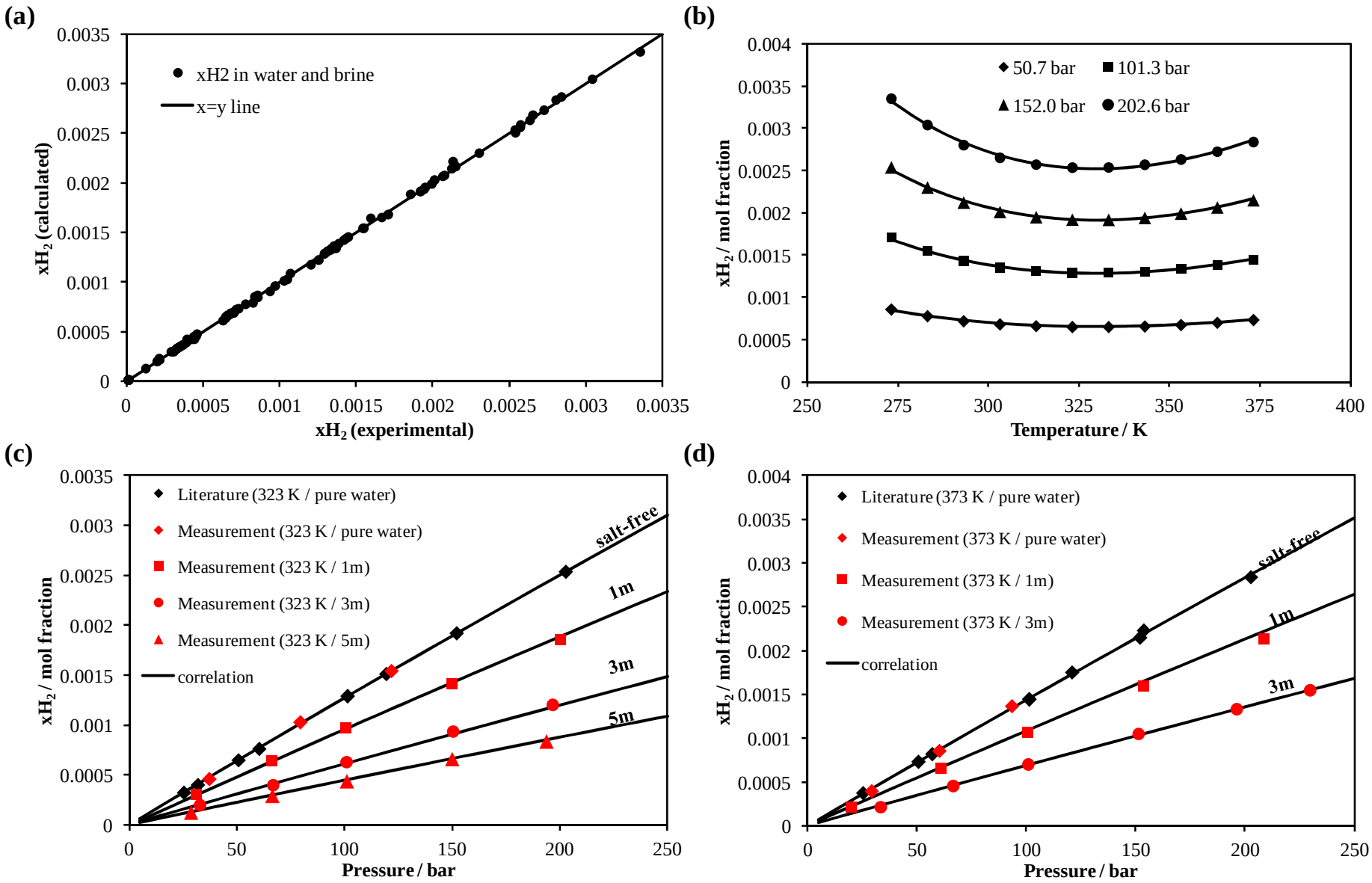

Figure 9: Calculated Solubility (solid lines) of H_2 in H_2O ± NaCl using correlation (Equations 12 and 13). (a): measured vs calculated x_{H_2}; (b): Isobars of H_2 solubility in pure water; (c) and (d): Isotherms of solubility of H_2 in water and brine at different molalities. Literature data [20, 49, 52] are represented by black symbols and measured ones (Table 4) are represented by red symbols.

4. Conclusions

Knowledge of high pressure hydrogen solubility in brine is of great importance especially for Underground Hydrogen Storage (UHS), however, a literature review has shown that there are no published experimental data at high pressure to date due to technical and safety challenges. The "static-analytic" apparatus developed and validated in our previous work has been used to perform original measurements of H_2 solubility in H_2O+NaCl at high pressure (up to 230 bar) and at different temperatures (323 and 373 K) and molality (from salt-free to highly concentrated NaCl brine). The GC calibration was verified by performing measurements of H_2 solubility in pure water which were compared with available literature data. The consistency of the measured data was verified with a Krichevsky-Kasarnovsky type approach. Some medium uncertainties were observed at low pressure (low solubility) due to the necessity of using two syringes of different volumes for calibration (one for small quantities and the other for large quantities). The new H_2 solubility data will serve to improve the models implemented in the various reservoir simulation software (e.g. the nonisothermal multiphase flow and reactive transport simulator OpenGeoSys [15]) for the simulation of hydrogen storage.

For the processing of these new measured data, three models (Geochemical, SW, and e-PR-CPA models) using different thermodynamic approaches were used. The new data were used in the parameterization of these models, and in the evaluation of recently published pseudo-data from molecular simulation or "predictive" models. The tested models can describe very well the solubility of H_2 in water and brine as well as the water content in the H_2-rich phase under different thermodynamic conditions. Accurate data tables of water content and H_2 solubility in H_2O±NaCl were generated with the e-PR-CPA model at different temperature, pressure and molality. Moreover, a simple Setschenow-type correlation has been proposed which is very efficient if used in the coefficient fitting range. Finally, the models and correlations proposed in this work can be used to calculate the solubility of hydrogen under geological storage conditions, however one method may be chosen over another, depending on the simplicity, accuracy, and degree of prediction (within or outside the fitting range).

Acknowledgments

Financial support from Géodénergies through the project "Rostock H" is gratefully acknowledged.

References

[1] Melaina MW, Antonia O, Penev M. Blending hydrogen into natural gas pipeline networks. a review of key issues. National Renewable Energy Laboratory; 2013.
[2] Shi Z, Jessen K, Tsotsis TT. Impacts of the subsurface storage of natural gas and hydrogen mixtures. International Journal of Hydrogen Energy. 2020;45:8757-73.
[3] Züttel A. Hydrogen storage methods. Naturwissenschaften. 2004;91:157-72.
[4] Ozarslan A. Large-scale hydrogen energy storage in salt caverns. International Journal of Hydrogen Energy. 2012;37:14265-77.
[5] Tarkowski R. Underground hydrogen storage: Characteristics and prospects. Renewable and Sustainable Energy Reviews. 2019;105:86-94.
[6] Bader N, Bleischwitz R, Madsen AN, Andersen PD. EU policies and cluster development of hydrogen communities. Bruges European Economic Research papers. 2008.
[7] Strobel G, Hagemann B, Huppertz TM, Ganzer L. Underground bio-methanation: Concept and potential. Renewable and Sustainable Energy Reviews. 2020;123:109747.
[8] Kruck O, Crotogino F. Benchmarking of selected storage options. Hannover, Germany. 2013.
[9] Crotogino F. Larger scale hydrogen storage. Storing energy: Elsevier; 2016. p. 411-29.
[10] Bai M, Song K, Sun Y, He M, Li Y, Sun J. An overview of hydrogen underground storage technology and prospects in China. Journal of Petroleum Science and Engineering. 2014;124:132-6.
[11] Reitenbach V, Ganzer L, Albrecht D, Hagemann B. Influence of added hydrogen on underground gas storage: a review of key issues. Environmental Earth Sciences. 2015;73:6927-37.
[12] Hagemann B, Rasoulzadeh M, Panfilov M, Ganzer L, Reitenbach V. Hydrogenization of underground storage of natural gas. Computational Geosciences. 2016;20:595-606.
[13] Lopez-Lazaro C, Bachaud P, Moretti I, Ferrando N. Predicting the phase behavior of hydrogen in NaCl brines by molecular simulation for geological applicationsPrédiction par simulation moléculaire des équilibres de phase de l'hydrogène dans des saumures de NaCl pour des applications géologiques. Bulletin de la Société Géologique de France. 2019;190.
[14] Bazarkina EF, Chou I-M, Goncharov AF, Akinfiev NN. The Behavior of H2 in Aqueous Fluids under High Temperature and Pressure. Elements: An International Magazine of Mineralogy, Geochemistry, and Petrology. 2020;16:33-8.
[15] Li D, Beyer C, Bauer S. A unified phase equilibrium model for hydrogen solubility and solution density. International Journal of Hydrogen Energy. 2018;43:512-29.
[16] Søreide I, Whitson CH. Peng-Robinson predictions for hydrocarbons, CO2, N2, and H2S with pure water and NaCl brine. Fluid Phase Equilibria. 1992;77:217-40.
[17] Chabab S, Théveneau P, Corvisier J, Coquelet C, Paricaud P, Houriez C, et al. Thermodynamic study of the CO2–H2O–NaCl system: Measurements of CO2 solubility and modeling of phase equilibria using Soreide and Whitson, electrolyte CPA and SIT models. International Journal of Greenhouse Gas Control. 2019;91:102825.
[18] Chabab S, Ahmadi P, Théveneau P, Coquelet C, Chapoy A, Corvisier J, et al. Measurements and modeling of high-pressure O2 and CO2 solubility in brine (H2O+NaCl). Fluid phase equilibria. 2020;submitted.
[19] Wiebe R, Gaddy V. The solubility of hydrogen in water at 0, 50, 75 and 100° from 25 to 1000 atmospheres. Journal of the American Chemical Society. 1934;56:76-9.
[20] Young CL. Hydrogen and deuterium. Solubility Data Series. 1981;5:428-9.
[21] Bunsen R. Ueber das Gesetz der Gasabsorption. Justus Liebigs Annalen der Chemie. 1855;93:1-50.

[22] Timofejew W. Über die Absorption von Wasserstoff und Sauerstoff in Wasser und Alkohol. Zeitschrift für Physikalische Chemie. 1890;6:141-52.
[23] Bohr C, Bock J. Bestimmung der Absorption einiger Gase in Wasser bei den Temperaturen zwischen 0 und 100°. Annalen der Physik. 1891;280:318-43.
[24] Winkler L. The solubility of gases in water (first treatise). Ber Dtsch Chem Ges. 1891;24:89-101.
[25] Steiner P. Ueber die Absorption des Wasserstoffs im Wasser und in wässerigen Lösungen. Annalen der Physik. 1894;288:275-99.
[26] Braun L. Über die Absorption von Stickstoff und von Wasserstoff in wässerigen Lösungen verschieden dissociierter Stoffe. Zeitschrift für Physikalische Chemie. 1900;33:721-39.
[27] Geffcken G. Beiträge zur kenntnis der löslichkeitsbeeinflussung. Zeitschrift für Physikalische Chemie. 1904;49:257-302.
[28] Knopp W. Über die Löslichkeitsbeeinflussung von Wasserstoff und Stickoxydul in wässerigen Lösungen verschieden dissoziierter Stoffe. Zeitschrift für Physikalische Chemie. 1904;48:97-108.
[29] Huefner G. Study of the absorption of nitrogen and hydrogen in aqueous solutions. Z Phys Chem Stoechiom Verwandtschaftsl. 1907;57:611-25.
[30] Findlay A, Shen B. CLVI.—The influence of colloids and fine suspensions on the solubility of gases in water. Part II. Solubility of carbon dioxide and of hydrogen. Journal of the Chemical Society, Transactions. 1912;101:1459-68.
[31] Müller C. Die Absorption von Sauerstoff, Stickstoff und Wasserstoff in wässerigen Lösungen von Nichtelektrolyten. Zeitschrift für Physikalische Chemie. 1913;81:483-503.
[32] Ipatiew W, Drushina‐Artemowitsch S, Tichomirow W. Löslichkeit des Wasserstoffs in Wasser unter Druck. Berichte der deutschen chemischen Gesellschaft (A and B Series). 1932;65:568-71.
[33] Morrison T, Billett F. 730. The salting-out of non-electrolytes. Part II. The effect of variation in non-electrolyte. Journal of the Chemical Society (Resumed). 1952:3819-22.
[34] Pray H. CE Schweickert u. BH Minnich. Ind Eng Chem. 1952;44:1146.
[35] Zoss L. A Study of the Hydrogen and Water and Oxygen and Water Systems at Various Temperatures and Pressures: Ph. D. thesis, Purdue University, West Lafayette, IN; 1952.
[36] Pray H, Stephan EF. The solubility of hydrogen in uranyl sulphate solutions at elevated temperatures. Battelle Memorial Inst., Columbus, Ohio; 1953.
[37] Wet Wd. Determination of gas solubilities in water and some organc liquids. JS Afr Chem Inst. 1964;17:9-13.
[38] Ruetschi P, Amlie R. Solubility of hydrogen in potassium hydroxide and sulfuric acid. Salting-out and hydration. The Journal of Physical Chemistry. 1966;70:718-23.
[39] Shoor S, Walker Jr RD, Gubbins K. Salting out of nonpolar gases in aqueous potassium hydroxide solutions. The Journal of Physical Chemistry. 1969;73:312-7.
[40] Longo LD, Delivoria-Papadopoulos M, Power GG, Hill EP, Forster 2nd R. Diffusion equilibration of inert gases between maternal and fetal placental capillaires. American Journal of Physiology-Legacy Content. 1970;219:561-9.
[41] Power GG, Stegall H. Solubility of gases in human red blood cell ghosts. Journal of Applied Physiology. 1970;29:145-9.
[42] Gerecke J, Bittrich H. The solubility of H2, CO2 and NH3 in an aqueous electrolyte solution. Wiss Z Tech Hochsch Chem Carl Shorlemmer Leuna Merseburg. 1971;13:115-22.
[43] Jung J, Knacke O, Neuschut D. Solubility of carbon monoxide and hydrogen in water at temperatures up to 300 degrees c. Chemie ingenieur technik. 1971;43:112-&.
[44] Schröder W. Untersuchungen über die Temperaturabhängigkeit der Gaslöslichkeit in Wasser. Chemie Ingenieur Technik. 1973;45:603-8.

[45] Crozier TE, Yamamoto S. Solubility of hydrogen in water, sea water, and sodium chloride solutions. Journal of Chemical and Engineering Data. 1974;19:242-4.
[46] Gordon LI, Cohen Y, Standley DR. The solubility of molecular hydrogen in seawater. Deep Sea Research. 1977;24:937-41.
[47] Cargill RW. Solubility of helium and hydrogen in some water+ alcohol systems. Journal of the Chemical Society, Faraday Transactions 1: Physical Chemistry in Condensed Phases. 1978;74:1444-56.
[48] Gillespie P, Wilson G. GPA Research Report RR-41 Gas Processors Association. Tulsa, OK. 1980.
[49] Choudhary VR, Parande MG, Brahme PH. Simple apparatus for measuring solubility of gases at high pressures. Industrial & Engineering Chemistry Fundamentals. 1982;21:472-4.
[50] Dohrn R, Brunner G. Phase equilibria in ternary and quaternary systems of hydrogen, water and hydrocarbons at elevated temperatures and pressures. Fluid phase equilibria. 1986;29:535-44.
[51] Alvarez J, Crovetto R, Fernández‐Prini R. The dissolution of N2 and of H2 in water from room temperature to 640 K. Berichte der Bunsengesellschaft für physikalische Chemie. 1988;92:935-40.
[52] Kling G, Maurer G. The solubility of hydrogen in water and in 2-aminoethanol at temperatures between 323 K and 423 K and pressures up to 16 MPa. The Journal of Chemical Thermodynamics. 1991;23:531-41.
[53] Jáuregui-Haza U, Pardillo-Fontdevila E, Wilhelm A, Delmas H. Solubility of hydrogen and carbon monoxide in water and some organic solvents. Latin American applied research. 2004;34:71-4.
[54] Taylor BN, Kuyatt CE. Guidelines for evaluating and expressing the uncertainty of NIST measurement results. 1994.
[55] Taylor BN. Guidelines for Evaluating and Expressing the Uncertainty of NIST Measurement Results (rev: Diane Publishing; 2009.
[56] Soo C-B. Experimental thermodynamic measurements of biofuel-related associating compounds and modeling using the PC-SAFT equation of state 2011.
[57] Zhang F. Développement d'un dispositif expérimental original et d'un modèle prédictif pour l'étude thermodynamique des composés soufrés: Paris, ENMP; 2015.
[58] El Abbadi J. Etude des propriétés thermodynamiques des nouveaux fluides frigorigènes: PSL Research University; 2016.
[59] Krichevsky I, Kasarnovsky J. Partial Molal Quantities in an Infinitely Dilute Solution. Journal of the American Chemical Society. 1935;57:2171-2.
[60] Corvisier J. Modeling water-gas-rock interactions using CHESS/HYTEC. Goldschmidt Conference, Florence–Italy2013.
[61] Corvisier J, Bonvalot A-F, Lagneau V, Chiquet P, Renard S, Sterpenich J, et al. Impact of co-injected gases on CO2 storage sites: Geochemical modeling of experimental results. Energy Procedia. 2013;37:3699-710.
[62] Blanc P, Lassin A, Piantone P, Azaroual M, Jacquemet N, Fabbri A, et al. Thermoddem: A geochemical database focused on low temperature water/rock interactions and waste materials. Applied geochemistry. 2012;27:2107-16.
[63] Harvey AH. Semiempirical correlation for Henry's constants over large temperature ranges. AIChE journal. 1996;42:1491-4.
[64] Shock EL, Helgeson HC, Sverjensky DA. Calculation of the thermodynamic and transport properties of aqueous species at high pressures and temperatures: Standard partial molal properties of inorganic neutral species. Geochimica et Cosmochimica Acta. 1989;53:2157-83.

[65] Schneider AC, Pasel C, Luckas M, Schmidt KG, Herbell J-D. Determination of hydrogen single ion activity coefficients in aqueous HCl solutions at 25 C. Journal of solution chemistry. 2004;33:257-73.
[66] Sakaida H, Kakiuchi T. Determination of single-ion activities of H+ and Cl–in aqueous hydrochloric acid solutions by use of an ionic liquid salt bridge. The Journal of Physical Chemistry B. 2011;115:13222-6.
[67] Khoshkbarchi MK, Vera JH. Measurement and correlation of ion activity in aqueous single electrolyte solutions. AIChE journal. 1996;42:249-58.
[68] Lemmon E, Bell IH, Huber M, McLinden M. NIST Standard Reference Database 23: Reference Fluid Thermodynamic and Transport Properties-REFPROP, Version 10.0. National Institute of Standards and Technology. 2018.
[69] Peng D-Y, Robinson DB. A new two-constant equation of state. Industrial & Engineering Chemistry Fundamentals. 1976;15:59-64.
[70] Wertheim M. Fluids with highly directional attractive forces. I. Statistical thermodynamics. Journal of statistical physics. 1984;35:19-34.
[71] Blum L. Mean spherical model for asymmetric electrolytes: I. Method of solution. Molecular Physics. 1975;30:1529-35.
[72] Born M. Volumen und hydratationswärme der ionen. Zeitschrift für Physik. 1920;1:45-8.
[73] Hajiw M, Chapoy A, Coquelet C. Hydrocarbons–water phase equilibria using the CPA equation of state with a group contribution method. The Canadian Journal of Chemical Engineering. 2015;93:432-42.